ELSEVIER

Ceramics International 32 (2006) 21–28

CERAMICS INTERNATIONAL

www.elsevier.com/locate/ceramint

In situ formation of Al_2O_3–SiC–mullite from Al-matrix composites

M.F. Zawrah [a,*], M.H. Aly [b]

[a] *National Researh Center, Ceramics Department, 12622 Dokki, Cairo, Egypt*
[b] *Institute of Desert Environmental Researches, Minufiya University, Sadat City, Minufiiya, Egypt*

Received 27 August 2004; received in revised form 12 November 2004; accepted 28 December 2004
Available online 24 March 2005

Abstract

Five composite batches (M1–M5) containing Al_2O_3–SiC–mullite–Al were designed and prepared in situ from different proportion mixtures of alumina, silicon carbide and aluminum alloy. The phase composition and microstructure were studied using X-ray diffraction (XRD) and scanning electron microscope (SEM) techniques. Sinterability in terms of bulk density, apparent porosity and compressive strength were also measured. All samples exhibit XRD reflections characteristic of alumina, SiC, and mullite. The amount of these phases depended on starting batch compositions, oxidation of Al-alloy, oxidation of SiC, and reaction of starting and oxidized materials together to form mullite. In the composites-containing lower mullite content, new silica-rich phase (aluminum silicate phase, i.e. $Al_2Si_4O_{10}$) and/or cristobalite appeared. The formed mullite or silica rich phase prevents further oxidation of SiC or Al–metal. These phase compositions reflect the higher density, lower porosity and good mechanical properties of such composites. The presence of low melting silicate phases was found to increase the bulk density and consequently to decrease the apparent porosity.

Keywords: B. Composites; D. SiC; D. Alumina; Advanced ceramics; Thermo-mechanical applications

1. Introduction

Alumina-based ceramic-matrix composites have shown promise as advanced materials for high-temperature applications because of their excellent refractoriness, low susceptibility to oxidation and good mechanical properties at elevated temperatures [1–5]. It is well known that composites based on corundum as well as other inorganic refractory compounds (carbides, nitrides, borides of transition metals) have generated considerable interest in scientific as well as technological literature [6]. In particular, these composites possess a combination of physical and mechanical properties which makes them attractive for a variety of applications. In choosing reinforcement for ceramic composites, SiC is definitely among the best. It exhibits attractive properties such as high modulus, high strength, good corrosion/oxidation resistance and good high-temperature strength. Ceramics reinforced with SiC show better mechanical properties than their monolithic counterparts [7]. Alumina, mullite and silicon carbide are prospective materials in the field of engineering ceramics due to their superior high temperature mechanical properties [8–13] and resistance toward chemical attack. But, these materials suffer from poor fracture resistance [14] which renders them unsuitable for applications in diverse fields. Fabrication of composite consisting of alumina, SiC and mullite, however to some extent is difficult and inert atmosphere during consolidation is always maintained to have a check on the oxidation of SiC [15]. Conventional process encompass pressureless sintering and hot pressing [16]. A newer fabrication route has been recently proposed. It involves reaction sintering of powder mixtures where metallic aluminum was along with SiC and the compact being sintered in air, the oxidation products of SiC, i.e. SiO_2 and aluminium, i.e. Al_2O_3 combining together to form mullite at higher temperature [17–18]. It is now established [19] that oxidation can be prevented if mullitisation takes place at such temperature where oxidation of SiC is not much. In the present work, alumina, SiC and aluminum metal were used to prepare a composite in which

* Corresponding author. Fax: +20 2 3370931.
E-mail address: mzawrah@hotmail.com (M.F. Zawrah).

0272-8842/$30.00
doi:10.1016/j.ceramint.2004.12.005

SiC particles are kept dispersed so that a uniform mullite phase is formed around SiC particles which will ultimately help in preventing further oxidation of SiC and form the mullite phase. Wu and Claussen [20] obtained compact of alumina and partially oxidized SiC (SiC particles with silica layers on the surfaces) by controlled oxidation of green compacts of Al and SiC powder mixtures. Then reaction sintering combined alumina and silica layers to form mullite. This process resulted in dense samples with high strength and low sintering shrinkage. Silicon carbide or alumina reinforced aluminum matrix composites have attracted considerable attention in recent years. These composites provide significant improvements in elastic modulus, wear resistance, and high-temperature mechanical properties for thermo-mechanical applications such as automotive and aerospace structures. The need for increasing strength and stiffness, and decreasing the weight of materials for transport and structural applications has recently attracted much interest in metal-matrix composites. They are generally produced by three techniques namely, powder metallurgy, stir casting and liquid metal infiltration [21]. The objective of this paper is to process composites of Al_2O_3–SiC–mullite–Al starting from Al-matrix composite. The obtained composites were investigated through studying their sinterability, phase composition, microstructure, and mechanical properties.

2. Experimental Procedures

The starting materials used in the present work were pure fine powders of calcined α-alumina (99.5% purity and <100 μm size), β-SiC (98% purity and 16 m^2/g surface area) and Al-alloy. Crystalline elemental powders were used in this study to prepare Al alloys with a nominal composition of $Al_{93}Fe_3Ti_2Cr_2$. The aluminum powder used had a purity of 99.5% with a mean particle size of 70 μm, while the corresponding values for iron, chromium and titanium powders were 99.0, 98.5 and 99.5% as well as 50, 30 and 30 μm, respectively.

Five composite batches were prepared from the starting materials according to their composition shown in Table 1. These mixes are designed as M1, M2, M3, M4 and M5. The composites were prepared by powder metallurgy technique. After mixing, batches of 12.7 mm diameter cylinders were prepared by semi-dry pressing under 80 MPa and polyvinyl alcohol as binder and then fired at 700 °C for 3 h [from thermo-gravimetric analysis (TGA), SiC powders would not significantly oxidize at this burnout temperature [7]] and then fired up to 1600 °C in air. After sintering, the presence of a few fine particles was observed on the surface of some samples due to the oxidation. The particles were found to be consisting mainly of alumina, SiC and $Al_2Si_4O_{10}$ phases. A Philips X-Ray Diffraction equipment model PW/1710 with Monochromator, Cu radiation (λ = 0.154 nm at 40 KV, 30 mA) and scanning speed 0.02 °/s was used to investigate experimentally the phase compositions of the fired composite batches. Physical properties namely; bulk density (BD), apparent porosity (AP) were tested using water displacement method (Archimedes' method). The phase composition and microstructure of the sintered composites were investigated by using scanning electron microscope (SEM) (model Philips XL 30 with an EDAX attached unit). Mechanical properties in terms of compressive strength were also assessed according to ASTM standard C133-91 and Egyptian standard 1859 (1990).

Table 1
Batch composition of the processed composites

Sample no.	Composition (wt.%)		
	Alumina	SiC	Al-alloy
M1	40	30	30
M2	35	35	30
M3	30	30	40
M4	15	45	40
M5	30	25	45

3. Results and discussions

3.1. Phase compositions

We have fabricated Al_2O_3–SiC–mullite–Al composites of various compositions by reaction sintering of alumina, SiC and Al alloy powder compacts. Since oxidation of SiC powders yielded silica ($SiC_{(s)} + 2O_{2(g)} = SiO_{2(s)} + CO_{2(g)}$), the initial amount of SiC powders and its oxidation extents determined the amounts of silica and residual SiC in the compacts after oxidation treatments. Also, the oxidation of Al–metal yielded alumina. Hence, with proper amounts of alumina, SiC and Al alloy in the starting powder mixtures and a careful control of oxidation treatment of the green compacts, we have been able to produce compacts consisting of alumina, SiO_2, Al–metal, and SiC with planned proportion. Subsequent reaction sintering of these compacts results in a reaction between alumina and silica to form mullite ($3Al_2O_3{\cdot}2SiO_2$) and to yield Al_2O_3–SiC–mullite–Al–metal composite with designed phase ratios. The formation of layers of mullite and/or silica prevented further oxidation of silicon carbide and Al–metal.

XRD patterns and data of the alumina–SiC–mullite composites fired at 1600 °C are given in Fig. 1 and Table 2. All samples exhibit reflections assigned to α-alumina, β-SiC, and mullite. The amount of mullite in M2 is lower than that in M1 and M4 (which exhibit peaks of cristoballite also), and minor in M3 and M5. With decreasing the amount of mullite, a new silica-rich phase (aluminum silicate, i.e. $Al_2Si_4O_{10}$) which is considered as the one with a layered triclinic structure formed at lower temperature [22] and which forms low melting compound in the presence of Fe, Ti, and Cr) starts to appear in M2, M3 and M5. These results indicate the complete reaction between Al_2O_3, either already present or produced from the oxidation of aluminum, with

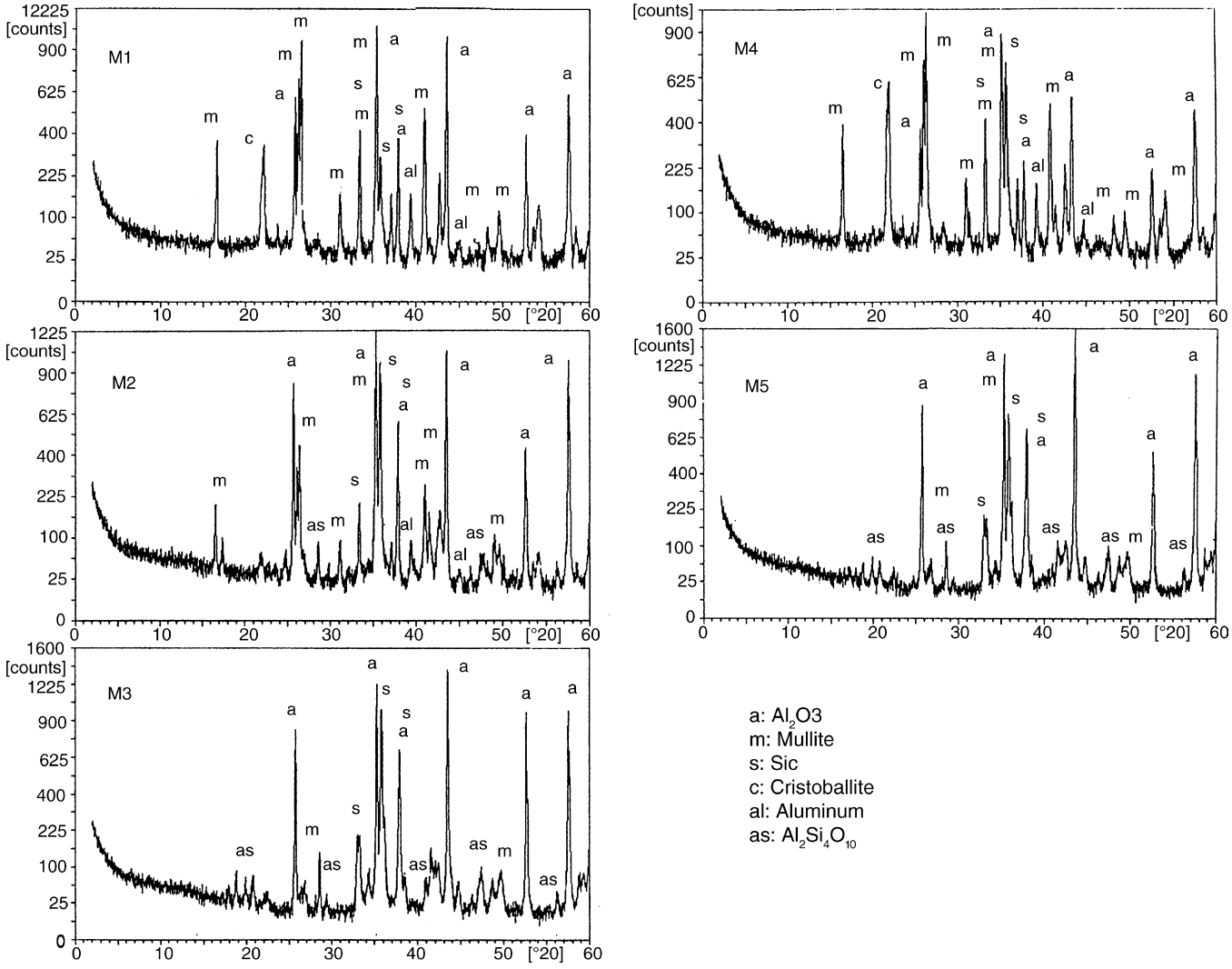

Fig. 1. XRD patterns of the processed alumina–SiC–mullite composites fired at 1600 °C.

SiO_2 produced from oxidation of SiC, in forming mullite and/or $Al_2Si_4O_{10}$. In M4, due to the higher-starting material-contents of SiC and Al–metal compared with alumina, the pattern of this sample shows lower peak intensity of α-Al_2O_3 and higher peak intensities of mullite, Al–metal and cristoballite. The sample M1 shows peak intensities of mullite, Al–metal and cristoballite relatively lower than those for M4. The maximum peak intensities of β-SiC are observed for the sample M2 and M3, while moderate peak intensities are formed for M4 and M5. The samples M2, M3, and M5 exhibit $Al_2Si_4O_{10}$ phase (not mullite phase) due to the reaction of cristoballite leading the formation of this phase and also to their relatively higher contents of not oxidized Al-alloy. The samples M4, M1 and M2 show the lower peak intensities of α-alumina as compared with M3 and M5, due to its reaction leading to mullite formation. The formed mullite or silica-rich phase prevents further oxidation of SiC or Al–metal. The in situ formed phases and their order of appearance in each sample as detected from intensities of XRD patterns, are also presented in Table 2.

Table 2
Formed phases and their ranking in each sample as detected from intensities of XRD patterns

Phases	Formation order of phases in each sample
Cristoballite	M1 and M4 > M2
$Al_2Si_4O_{10}$	M3 and M5 and M2
Mullite	M1 and M4 > M2 > M3 and M5
SiC	M2 and M3 > M4 and M5 > M1
Al_2O_3	M5 > M3 > M1 and M2 > M4
Al–metal	M4 > M1 > M2

The phase evolution and mullitisation processes in these samples were analogous to those reported in the reaction sintering of alumina and amorphous silica by sol–gel methods [22]. The silica layer resulting from SiC oxidation was essentially the same as silica particles or silica coating obtained from sol–gel process. Mullite was the dominant silicate phase when sintering temperatures were ≥1450 °C. Unreacted SiC cores were inert in the phase evolution. The mechanism of mullite formation from reaction of alumina

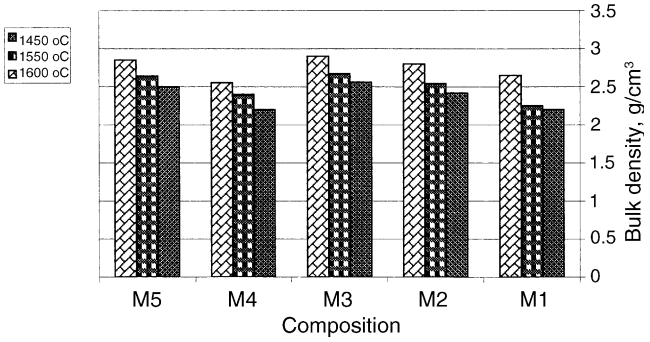

Fig. 2. Bulk density of the sintered composites at different firing temperatures.

and amorphous silica was believed to be via nucleation and growth from the siliceous matrix in which alumina dissolved and diffused through, to reach the saturation composition for mullite nuclei. Accordingly, the easier the alumina dissolved into and diffused through the silica glass, the easier the mullite would form [23].

3.2. Sinterability of the composites

Since the composite samples were mainly composed of alumina–SiC–mullite–Al with another minor phases, their bulk density was measured after having been sintered up to 1600 °C for 2 h, and plotted in Fig. 2 against composition. Fig. 2 clearly shows that both composition of the composite and firing temperature affected the densification process. As the firing temperature increases, the bulk density increases and consequently the apparent porosity decreases (Fig. 3). M4 exhibits the lowest bulk density among all composite batches due to its lower contents of alumina and higher contents of mullite and Al-alloy. M1 shows higher bulk density and apparent porosity than M4, due to its higher contents of alumina. In spite of its higher bulk density, it shows higher porosity, so it required higher sintering temperature to decrease the apparent porosity. The presence of higher contents of cristoballite, Al–metal and mullite in M1 and M4 could not significantly improve the densification as compared with M2, M3 and M5. This seems to be due to the thermal expansion mismatch and lower density of these

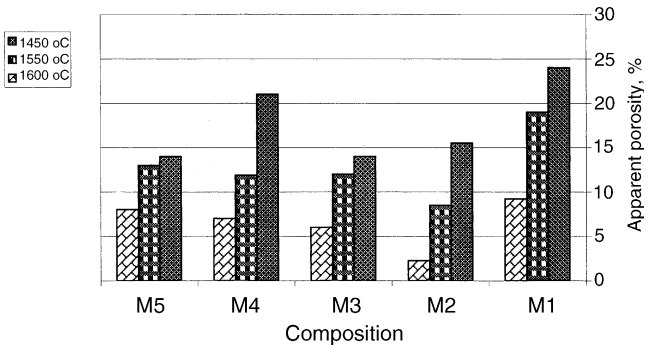

Fig. 3. Apparent porosity of the sintered composites at different firing temperatures.

phases. Also, it is well known that mullite has a very poor sinterability and could only be sintered to near theoretical density at 1600–1700 °C [24,25]. The presence of higher contents of alumina, SiC with low melting silicate phases increase the bulk density and consequently decrease the apparent porosity of M2, M3 and M5 (Figs. 2 and 3).

The sintered samples showed little volume changes because both expansion and contraction process proceeded simultaneously with the possibility of obtaining a sintered material with low to no volume change. Volume expansion can be explained on the basis of the formation of SiO_2 from SiC and conversion of SiO_2 to mullite, both leading to volume expansion. But it was found that by increasing Al_2O_3 content of the specimens volume changes decrease [8]. Due to the thermal stress produced from the thermal expansion mismatch during and after phase formation, some micro cracks are formed in M4.

3.3. Microstructure

In order to study the morphology of reaction products and to identify the corresponding chemical composition, SEM and EDS analyses were carried out on the Al_2O_3–mullite–SiC–Al composites sintered at 1600 °C. The properties of the particulate composites are controlled by the properties of

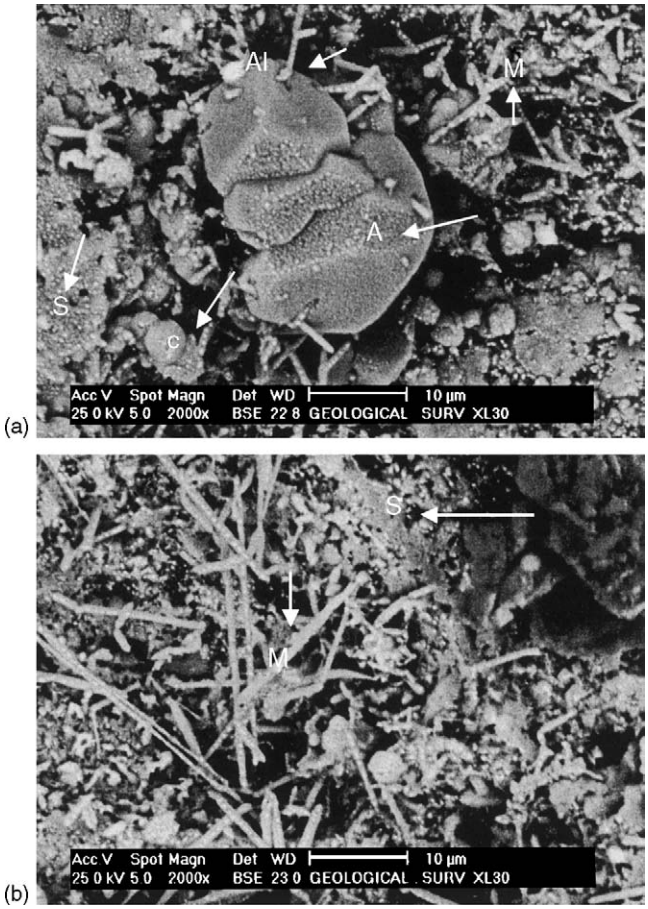

Fig. 4. SEM photomicrographs of sintered M1 composite.

the matrix and the reinforcement, the grain size of the matrix, the porosity content of the composites, the volume fraction and distribution of the reinforcing particles and phases formed at the particle interfaces or within the grains. Therefore, in the produced composites, some of these structural parameters, such as porosity content, phase distribution and composition were investigated. SEM micrographs of sintered composites and their EDS analyses are shown in Figs. 4–11. Fig. 4 exhibits the micrograph of M1. Rounded sphere crystals of cristobalite (point C) with hexagonal and facetted crystals of alumina (point A) with grain size of about 10–15 μm are observed in Fig. 4a. On the other hand, white–gray elongated grains of mullite are appeared in Fig. 5a and b (point M), which is confirmed by the EDS data (Fig. 5). Both SiC and Al–metal (white) with their round and small grain sizes (about 0.5–1 μm) are appeared in both photographs (points S and Al, respectively). Fine crystallized alumina grains, of few nanometers, distributed in all micrograph are present (white). This structure confirms also the porosity obtained from the densification parameters. Compact and dense microstructure was obtained for M2 as shown in Fig. 6a and b. A little amount of rounded crystals of Al–metal with moderate amount of elongated mullite crystals are apparent in this micrographs (point M). Well-defined small grains of SiC (point S) with grain size of about 0.5–1 μm and coarse grain (10 μm) of alumina (point A) direct-bonded together are present in this structure. The total area qualitative microanalysis of this sample is shown in Fig. 7. Relatively different microstructures are obtained for M3 (Fig. 8) with three main phases. Fig. 8 clearly shows the presence of irregularly-shaped SiC particles (gray; point S) randomly distributed with lightest fine or coarse alumina crystals (point A) with grain sizes of few nanometers or 10–20 μm, respectively. A white well defined-shape phase is also observed in this micrograph (Fig. 8b). The qualitative point analysis of this phase is shown in Fig 9. According to the displacement reaction ($3SiO_2 + 4Al = 2Al_2O_3 + 3Si$), all

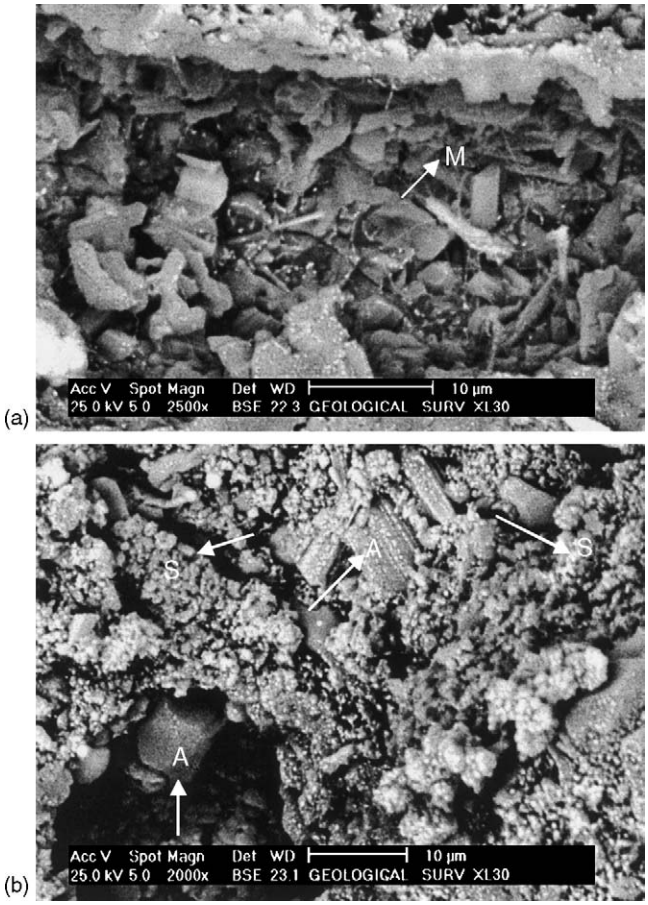

Fig. 6. SEM photomicrographs of sintered M2 composite.

SiO_2 is consumed within sufficient time, and the Si is dissolved in the liquid Al within the composite [26]. Following the reaction, the Si that is displaced from the SiO_2 preform diffuses out of the newly formed composite along the Al channels to the surrounding bath forming $Al_2Si_4O_{10}$ phase. Micrographs of M4 are shown in Fig. 10. They support the presence of an elongated mullite phase (point M)

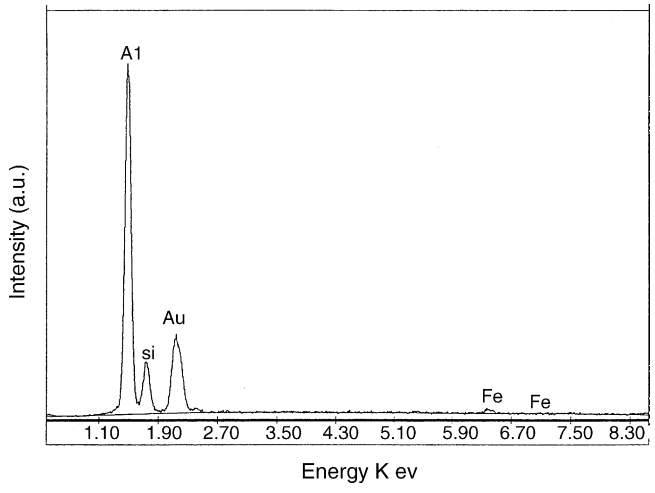

Fig. 5. EDS analysis of elongated grains in M1 composite.

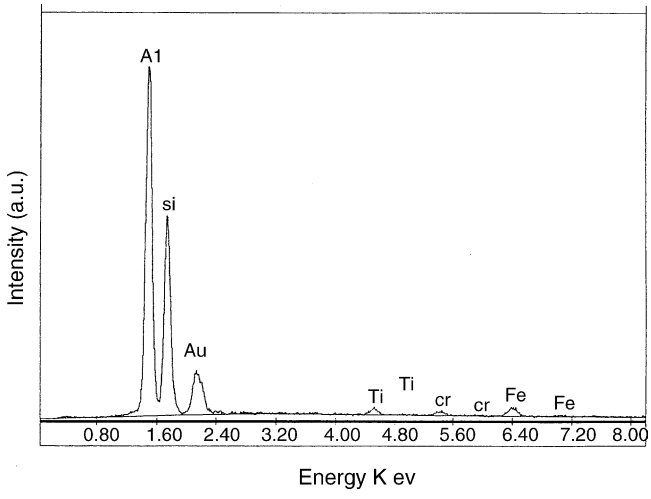

Fig. 7. Total area EDS analysis of sintered M2 composite.

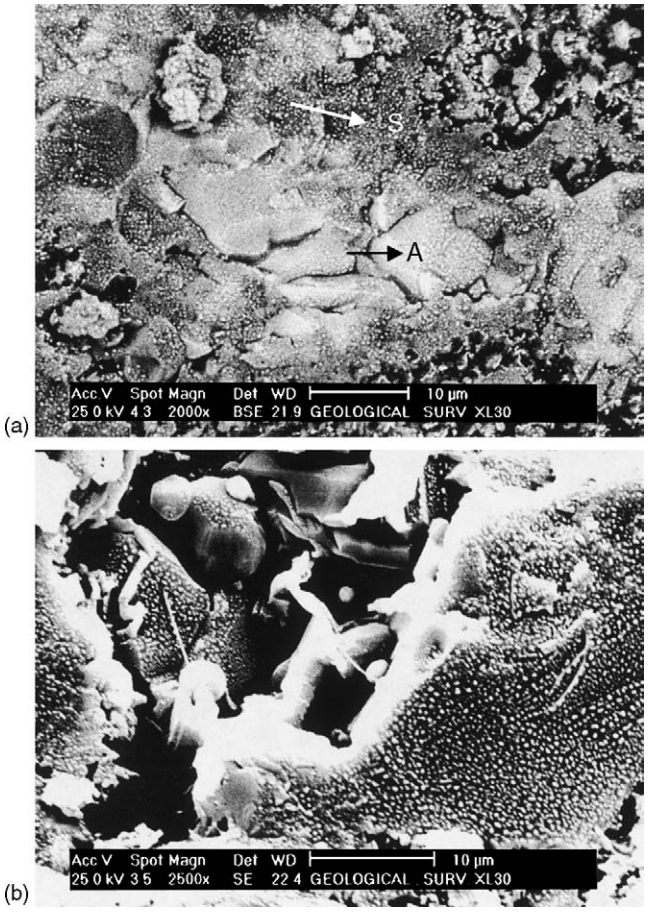

Fig. 8. SEM photomicrographs and EDS analysis of sintered M3 composite.

Fig. 10. SEM photomicrographs of sintered M4 composite.

formed around spherical small and fine crystals of SiC (gray; point S), cristobalite (point S) and Al–metal (white; point Al). Fine and coarse grains of alumina (point A) are also detected in this micrograph. M5 microstructure (Fig. 11) show well compact and dense microstructure composed mainly of hexagonal α-alumina crystals (point A) bonded by rounded fine silicon carbide (point S). Both β-SiC and α-alumina crystals are surrounded by a thin-layer of silica-rich aluminum phase. The presence of such developed microstructure improves the other investigated properties such as the densification and mechanical properties. It is worthy to state that, when Al–metal is heated in air, it oxidizes to small new Al_2O_3 crystallites, which sinter and thereby bond together the originally added Al_2O_3 or ceramic particles as exhibited in all micrographs.

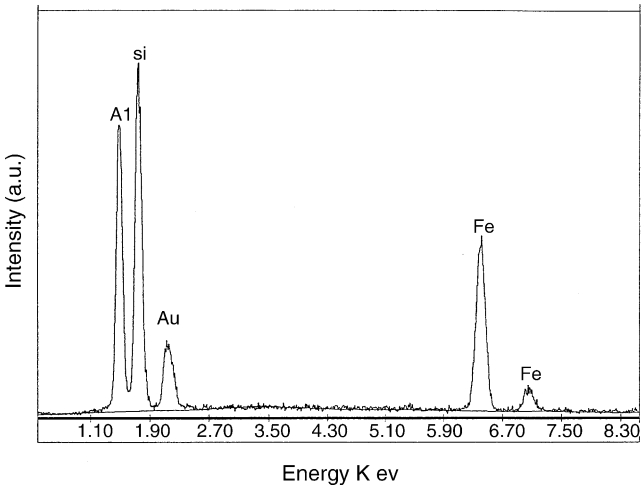

Fig. 9. EDS analysis of white phase in M3 composite.

3.4. Mechanical properties

Microstructure refining, shape, size, phase composition and porosity of the prepared composites, in addition to Young's modulus and residual stress strengthening effects correlated with SiC addition are the most important reasons accounting for the strength improvements. The formation of dislocation networks in the matrix grain boundaries also contributes to its strength increase [27]. Fig. 12 shows the compressive strength of the sintered composites at different firing temperature. It appears that the compressive strength increases as the firing temperature increases. The maximum strength is detected for the sample M2 and M5 due to their dense and compact microstructure. M2 is composed mainly of SiC, alumina, mullite and little amount of aluminum silicate ($Al_2Si_4O_{10}$) and Al–metal. On the other hand, M5

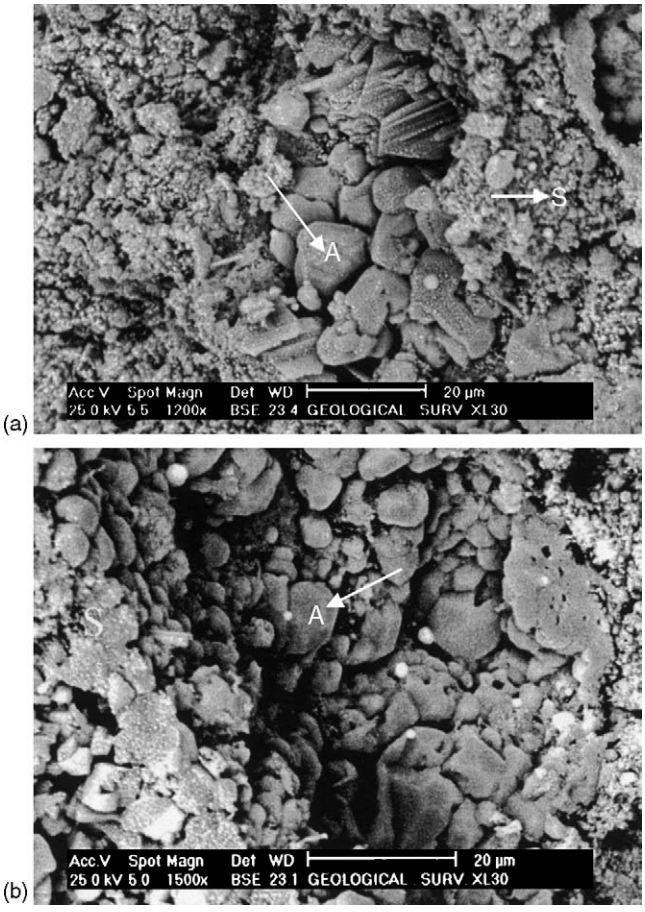

Fig. 11. SEM photomicrographs of sintered M5 composite.

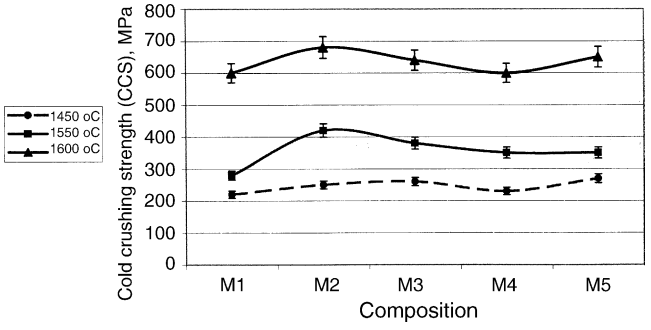

Fig. 12. Mechanical properties of the sintered composites at different firing temperatures.

has a lower porosity and contains higher SiC, alumina phases, in addition to aluminum silicate ($Al_2Si_4O_{10}$) which help to increase the strength. The presence of mullite in M1 and M4 relatively increases their strength after firing to 1600 °C.

4. Conclusion

It is concluded that all samples exhibit XRD reflections characteristic of α-alumina, β-SiC, and mullite. The amount of mullite in M2 is lower than that in M1 and M4 (which exhibit peaks of cristoballite also), and minor in M3 and M5. With decreasing the amount of mullite, a new silica-rich phase (aluminum silicate phase, i.e. $Al_2Si_4O_{10}$ starts to appear in M2, M3 and M5. The maximum peak intensities of β-SiC are observed for the samples M2 and M3, while the moderate peak intensities are found for M4 and M5. The samples M4, M1 and M2 show the lower peak intensities of α-alumina as compared with M3 and M5, due to its reaction to form mullite. The formed mullite or silica rich phases prevent further oxidation of SiC or Al–metal. These phase compositions reflect the higher density, lower porosity and good mechanical properties of M5, M3 and M2 composites.

References

[1] L.C. Pathak, D. Bandyopadhay, S. Srikanth, S. Kumar, P. Ramahandraarao, Effect of heating rates on synthesis of Al_2O_3–SiC composite by the self-propagating high-temperature synthesis (SHS) technique, J. Am. Ceram. Soc. 84 (5) (2001) 915–920.
[2] C. Wei, P.F. Becher, Development of SiC whisker reinforced ceramics, Am. Ceram. Soc. Bull. 64 (2) (1985) 298–304.
[3] T.N. Tieges, P.F. Becher, Sintered Al_2O_3–SiC whisker composites, Am. Ceram. Soc. Bull. 66 (2) (1987) 339–342.
[4] J. Homeny, W.L. Vaughn, Silicon carbide whisker–alumina composites; effect of whiskers surface treatment on fracture toughness, J. Am. Ceram. Soc. 73 (2) (1990) 394–402.
[5] J. Zhao, L.C. Steans, M.P. Harmer, H.M. Chan, G.A. Miller, R.F. Cook, Mechanical behavior of alumina–silicon carbide nanocomposites, J. Am. Ceram. Soc. 76 (2) (1993) 503–510.
[6] L.S. Aboyon, H.H. Nersisyan, S.L. Kharatyan, R. Orru, R. Saiu, G. Cao, D. Zedda, Synthesis of alumina–silicon carbide composites by chemically activated self-propagating reactions, Ceram. Int. 27 (2001) 163–169.
[7] Y.-J. Lin, C.-P. Tsang, The effect of starting precursors on the carbothermal synthesis of SiC powders, Ceram. Int. 29 (2003) 69–75.
[8] A.K. Samanta, K.K. Dhargupta, S. Ghatak, Near net shape SiC–mullite composites from a powder precursor prepared through an intermediate Al-hydroxyhydrogel, Ceram. Int. 27 (2001) 195–199.
[9] T.J. Whalen, Processing and properties of structural silicon carbide, Ceram. Eng. Sci. Proc. 7 (7–9) (1986) 1135–1143.
[10] G.C. Wei, P.F. Beher, Improvement in mechanical properties in SiC by addition of TiC particle, J. Am. Ceram. Soc. 647 (8) (1984) 571–574.
[11] M.A. Janney, Microstructural development and mechanical properties of SiC and SiC–TiC composites, Am. Ceram. Soc. Bull. 65 (2) (1986) 357–362.
[12] W.H. Gu, K.T. Faber, R.W. Steinbreech, Microcracking and R-curve behavior in SiC–TiB_2 composites, Acta Metall. Mater. 40 (11) (1992) 3121–3128.
[13] M.A. Janney, Mechanical properties and oxidation behaviour of a hot pressed SiC–15% vol. TiB_2 composites, Am. Ceram. Soc. Bull. 66 (2) (1987) 322–324.
[14] P. Chantikul, G.R. Anatis, B.R. Lawn, D.B. Marshall, A critical evaluation of indentation technique for measuring fracture toughness. II. Strength method, J. Am. Ceram. Soc. 64 (9) (1981) 539–543.
[15] M.I. Osendi, B.A. Bender, D. Lewis III, Microstructure and mechanical properties of mullite–silicon carbide composites, J. Am. Ceram. Soc. 72 (6) (1989) 1049–1054.
[16] J.W. Milewski, Efficient use of whisker in the reinforcement of ceramics, Adv. Ceram. Mater. 1 (1) (1986) 36–41.

[17] H. Kamiaki, C. Yamagishi, J. Asaumi, Mechanical properties and microstructure of mullite–SiC–ZrO_2 particulate composites, in: R.F. Somiya, J.A. Pask Davis (Eds.), Ceramic Transactions, vol. 6: Mullite and Mullite Matrix Composites, Am. Ceram. Soc., Westerville, OH, 1987, pp. 509–518.
[18] S. Wu, N. Claussen, Fabrication and properties of low-shrinkage reaction-bonded mullite, J. Am. Ceram. Soc. 74 (1991) 2460–2463.
[19] A.K. Samanta, K.K. Dhargupta, S. Ghatak, Retention of SiC during development of SiC–$M_xSi_yO_z$ composites {M = Al, Zr, Mg} by reaction bonding in air, J. Eur. Ceram. Soc. 20 (12) (2000) 889–1894.
[20] S. Wu, N. Claussen, J. Am. Ceram. Soc. 80 (1995) 1579.
[21] N. Altinkok, A. Demir, I. Ozsert, Processing of Al_2O_3/SiC ceramic cake preforms and their liquid Al–metal infiltration, Composites, Part A 34 (2003) 577–582.
[22] JCPDS-International Center for Diffraction Data, version 2.15, TU-Belrlin Inst. Fur Anorg. Analyt. Chemie, PDF-2 Database (sets 1–44) 1987–1994, Newtown Square, PA 19073, USA.
[23] M. Sacks, N. Bozkurt, G.W. Scheiffele, J. Am. Ceram. Soc. 74 (1991) 2428.
[24] O. Hirohi, K. Toshi, N. Atsushi, K. Niihara, J. Ceram. Soc. Jpn. 98 (1990) 541–547.
[25] M. Ismail, N. Zenjiro, Shigeyuki, J. Am. Ceram. Soc. 70 (1987) C7–C8.
[26] M.Y. Chen, M.C. Breslin, Friction behavior of co-continuous alumina/aluminum composites with and without SiC reinforcement, Wear 249 (2002) 868–876.
[27] L. Gao, X. Jin, H. Kawaoka, T. Sekino, K. Niihara, Microstructure and mechanical properties of SiC–mullite nanocomposites prepared by spark plasma sintering, Mater. Sci. Eng. A334 (2002) 262–266.